Dynamical disparity between hydration shell water and RNA in a hydrated RNA system

Debsindhu Bhowmik, P. Ganesh, Bobby G. Sumpter, and Monojoy Goswami

Phys. Rev. E **98**, 062407 — Published 14 December 2018

DOI: 10.1103/PhysRevE.98.062407

Dynamical disparity between hydration shell water and RNA in hydrated RNA system

Debsindhu Bhowmik

Computational Sciences and Engineering Division

P. Ganesh

Center for Nanophase Material Sciences

Bobby G. Sumpter and Monojoy Goswami*

Center for Nanophase Material Sciences and

Computational Sciences and Engineering Division,

Oak Ridge National Laboratory, Oak Ridge, TN, 37831

Abstract

We have performed large-scale molecular dynamics simulations on hammerhead RNA in water and observed disparity in the dynamical properties between water and RNA. The simulations are carried out above the dynamical transition temperature of RNA and is varied from below freezing to ambient temperature. Using this model, we observed different types of relaxation dynamics for water and RNA. While RNA shows a single stretched exponential decay, the water molecules show a double-exponential decay. Both water and RNA dynamics show temperature and spatial dependence on relaxation times. The RNA relaxations are many order of magnitude slower compared to water for all temperature and spatial length-scales. RNA relaxations show predominantly heterogeneous dynamics. Water dynamics in the hydration shell show a combination of interfacial water and bulk-like water properties and the water dynamics are decoupled from the RNA dynamics. These results explain the dynamics of water in the hydration shell and that of RNA.

PACS numbers: 87.10.ap,87.10.-e,82.39.Pj,76.60.-k

* goswamim@ornl.gov

I. INTRODUCTION

Most of the biological processes, involving the fundamental building blocks RNA and DNA, occur in aqueous environment. Water concentration around the biological molecules influence their structure, function and dynamics significantly [1–4]. The structural and dynamical properties of water near the biomolecules surface differ considerably from bulk water [5–7]. Water near the biomolecular surface, called the hydration shell, show unusual structural and dynamical properties [8, 9]. The hydration shell, consisting of the first few layers of water molecules, shows interesting water properties that are considerably different from water far away from the hydration shell. Hence, water dynamics in association with RNA is critical for fundamental understanding of biomolecular applications. The major challenge lies in distinctively identifying and differentiating the structural and dynamical properties of water in the hydration shell from the bulk [1].

The current growth of RNA based nanotechnology and drug-delivery system necessitates a comprehensive outlook of the properties at the molecular level [10, 11]. Structural and dynamical properties of RNA are highly dependent on hydration level, and water plays a crucial role in modifying RNA dynamics and its functions [12]. Apart from that the physical properties of RNA within the solvation shell, in general, is not well-understood and hence hinders the progress in RNA nano-biotechnology.

The water dynamics in the hydration shells can be characterized based on their residence times within the shell [13, 14]. The slowest water molecules are strongly bound to the biomolecular surface, while the more mobile water molecules form an interfacial layer. The third category of water molecules moves in and out of the solvation shell and act like bulk water. Recently, we have shown that by introducing nanodiamond, we can modify the water dynamics near the hydrated RNA surface, thereby triggering a different set of controlled RNA motion [15].

Experimental and theoretical studies confirm that the dynamics of biological macromolecules are often controlled by solvent dynamics [16–18], Recently, it has been shown that the dynamics of water away from the RNA surface is essential for the increased anharmonic motion of RNA with temperature increase [19]. Using neutron scattering and dielectric relaxation techniques, Khodadadi et al. [20] have examined a coupled relaxation dynamics of tRNA and water. While their experimental techniques represented a clearer understanding of tRNA-water dynamics, simulation based techniques can be more suitable for examining water relaxation in detail rather than expriments as water is often deuterated in the neutron experiments. In the present work, we overcome

the issue of deuterated water dynamics by using MD simulation that can seperately examine water and RNA dynamics from MD trajectories. This approach of investigating both water and RNA separately show differences in relaxation behavior between water and RNA dynamics that has not been observed earlier experiments.

Extensive amount of work on the dynamical transition temperature, T_D [21–23], of RNA molecules has been carried out in the past [12, 24–26]. In particular, Kührova et al [7] performed MD simulations to understand effect of specific choice of water model affecting the structure of A-RNA helical structures. In this work, however, we focus on the water dynamics in the hydration shell and the associated RNA dynamics that render unusual water behavior in the hydration shell above T_D. We approach the problem by investigating the dynamical aspects of water and RNA molecules using all-atom molecular dynamics simulations. Results are analyzed with regard to Quasi Elastic Neutron Scattering (QENS) experiments [27, 28]. We examine the water and RNA dynamics by invoking theories of water and polymer dynamics in confined phase [7, 29, 30]. We calculate the completely uncoupled relaxation dynamics from scattering profiles of RNA and water. The dynamical mismatch between RNA and water can be reconciled by invoking the physics of molecular relaxation in a confined space. The results are compared with previous studies on biomolecular relaxation and any discrepancies are further explained from the perspective of polymer dynamics.

II. SIMULATION DETAILS

Molecular Dynamics (MD) simulations were performed on D_2O hydrated hammerhead RNA systems. We choose hammerhead RNAs for this simulation as it typically serves as a model system for research in understanding the structure and dynamical properties of generalized RNA [19]. The initial coordinates for hammerhead RNA were taken from the protein data bank (PDB: 299D). The hydration level, h, in the D_2O hydrated hammerhead RNA corresponds to typical experimental level hydration, $h = 0.5$ (gm D_2O per gm of RNA) [15]. We used NAnoscale Molecular Dynamics (NAMD) simulation package [31] to perform the large-scale simulations. To construct the initial structure, a single RNA is placed into a pre-equilibrated box (shown in Figure 1(a)) of water eliminating the overlapping water molecules and is replicated into 8 (eight) identical RNAs for the full system. The full system with 8 identical RNAs are shown in Figure 1(b). All the RNA molecules and water interact with each other. Charge neutralization was achieved by adding

sodium ions. Each of the eight RNA molecules, the ions and water are rotated by a random angle around a randomly chosen principal axis to generate a fully random all-atom initial simulation structure. The simulation box sizes initially are $73.0 \times 66.4 \times 66.2 \text{Å}^3$ for all systems, and remained close to this value during the NPT simulations. Simulations were performed on both systems using the CHARMM-27 [32] protein nucleic acid force field and TIP3P [33] water model. Periodic boundary conditions (PBC) were used in all the dimensions. The long-range electrostatic interactions were calculated using Particle Mesh Ewald (PEM) method. The short-range interactions were calculated with a cutoff 12Å. Prior to data collection runs, the total energy of the systems was minimized and the systems were equilibrated for 6ns in NPT (isothermal-isobaric) ensemble at five different temperatures, $T = 260K$, $270K$, $280K$, $290K$ and $300K$. The deuteration of water was done during dynamical analysis using nMoldyn [34], a standard package to calculate transport properties from MD simulation trajectories commensurate with data obtained from neutron experiments. After equilibration, the statistical quantities were obtained from simulation runs of 10ns at each temperature with a time step of 1fs.

III. RESULTS AND DISCUSSION

The 10ns production runs were analyzed using VMD [35] software, nMoldyn [34] and our in-house analysis code to investigate the dynamics of the water and the hammerhead RNA molecules. The relaxation dynamics of the RNA and water molecules are examined for different scattering wave vectors, Q, and temperatures, T, ranging from $260K$ to $300K$. The wave vector, Q ($= 2\pi/\ell$, where ℓ is the length scale), ranges from 0.1Å^{-1} to 1.9Å^{-1} representing a wide range of length scales from 3.3Å to 62.8Å associated with molecular and the central simulation box length scales. While this article focuses on the dynamics of water and RNA molecules by investigating the diffusive and relaxation behavior of both RNA and water molecules, we briefly mention the structure of the water molecules near the RNA surface and bulk. The structures of water molecules at low and high temperatures around a single RNA molecule are shown in Figure 1(a) and the full system with 8 RNA molecules with hydration level, $h = 0.5$ are shown in Figure 1(b). The radial distribution functions (RDF), $g(r)$, are shown in Figures 1(c) and (d). Structurally water shows no difference between bulk and $g(r)$ near RNA surface for two different temperatures, $T = 270K$ and $300K$, except higher agglomeration in the bulk water as determined by the peak height of the $g(r)$. We define the interface and the bulk as 5Å near or away from the RNA surface. The

typical hydrogen bond (O-H) and O-O and H-H bonds are present in both of these cases. The different species of water RDF near the RNA surface (Figure 1(c)) show weaker agglomeration compared to the bulk (Figure 1(d)) at both low ($T = 270K$, solid lines) than at higher temperature ($T = 300K$, dashed lines). The higher agglomeration at bulk can be seen from the stronger RDF peaks in Figure 1(c) than Figure 1(d). There is a very little difference in peak heights with temperatures as can be observed from the $T = 270K$ (solid lines) and $T = 300K$ RDF plots. At these temperatures the water molecules are in liquid state at a very low density ($h = 0.5$) and hence show liquid water structures at both these temperatures, $T = 270K$ and $300K$. Therefore, no substantial changes in structures is observed, except a higher but very weak agglomeration at higher temperature. It should also be noted that the central simulation cell is relatively small, and the effects of the system size should be considered in further calculations. The bulk water, defined as 5Å away from the RNA surface, may be relatively closer to RNA surface that may deviate from a stringent definition of *bulk water*. As the central theme of this work is relaxation dynamics, we will not elaborate on the structures any further. However, we take into account the system size effect while calculating the dynamical properties in the following sections.

In the following, we will discuss the dynamics of the hydrogen (H) of RNA and deuterated water by investigating the mean square displacement (MSD) and the intermediate scattering function, $S(Q, t)$. In neutron experiments, the hydrogen atom (H-atom) dynamics of biomacromolecules can be observed. The biomacromolecular motions are mostly reflected in the dynamics of H-atom due to the abundance of the H-atom. Our choice of investigating the hydrogen dynamics stems from the neutron experiment setup. Furthermore, the water dynamics is calculated for all the waters of the system. Due to small system size, it is hard to distinguish between water on the RNA surface and water in the bulk, therefore it is imperative to study all the water dynamics together as discussed earlier.

The intermediate scattering function, $S(Q, t)$ are shown in Figure 2 for both the RNA and water H-atoms at two different temperatures, $T = 270K$ and $T = 300K$ for all the Q values to demonstrate the length-scale dependence of the structural relaxation. In neutron experiments, the scattering cross-section of deuterium is much weaker than H-atoms and hence deuterium labeling is a powerful technique to investigate the motion of complex biomolecule systems. In this study, consistent with the neutron scattering experiments, $S(Q, t)$ was calculated for RNA H-atoms only while treating water deuterated. The advantage of MD simulation [36] is that the deuterated water dynamics can also be obtained, which is otherwise not observed in neutron experiments. The

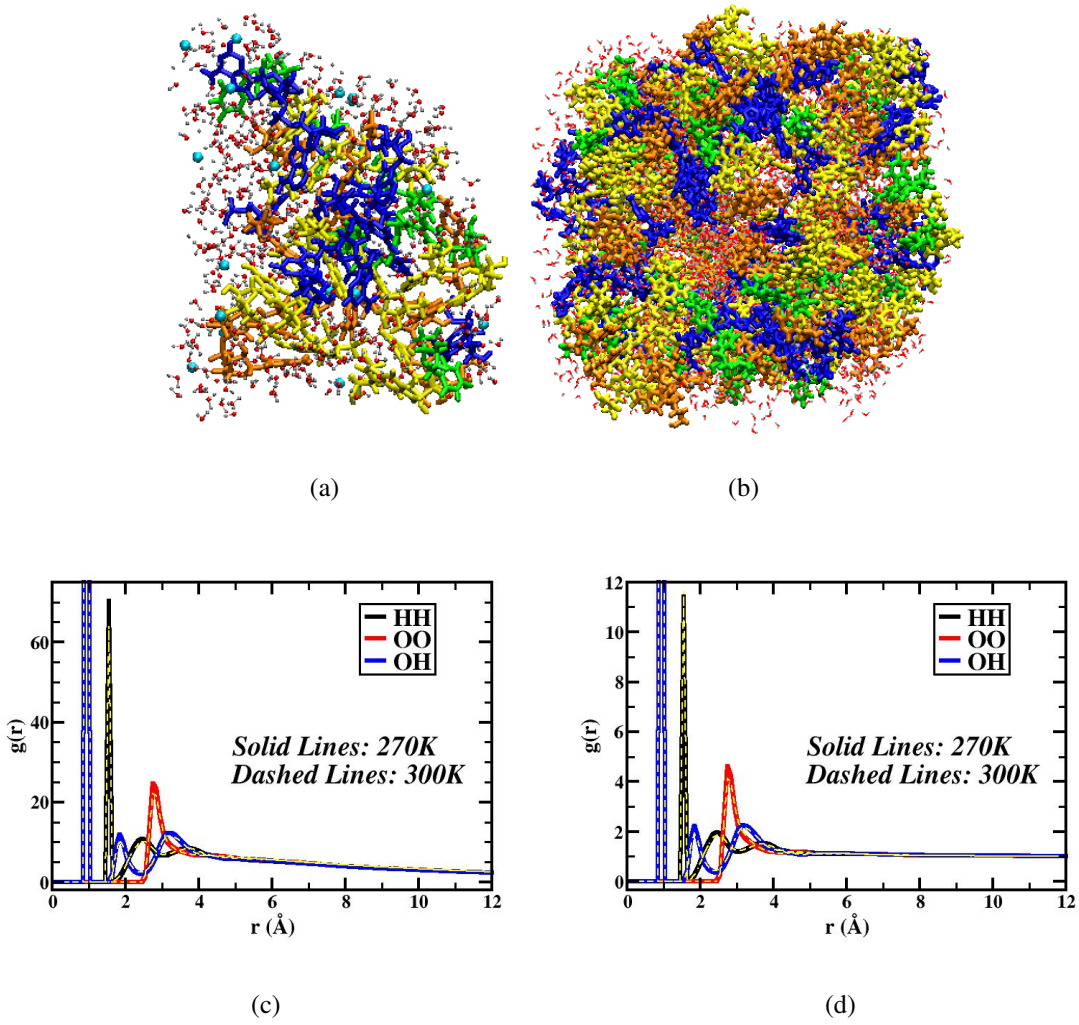

FIG. 1. Snapshot at the end of MD simulation. Only one RNA molecule at $T = 270K$, and the interfacial waters are shown in (a). (b) The full system at $T = 300K$ is shown. (c) and (d), radial distribution function, $g(r)$ of water inside the bulk and interfacial water near the surface respectively at temperatures, $T = 270K$ and $T = 300K$.

wave vector, $|Q| = 2 \times \pi/\ell$ where ℓ is the length scale of the observation. For the lowest and highest Q values, $Q = 0.1$Å for $Q = 1.9$Å refers to $\ell = 62.83$Å and 3.3Å respectively. Faster relaxation dynamics is observed in both the systems as Q increases. The relaxation dynamics at shorter length scale (higher Q) corresponds to the atomic scale dynamics while the longer length scale (lower Q) corresponds to the whole system, which is larger than the RNA molecule. As the length scale decreases, i.e., Q increases, the motion of the molecules become slower. Relaxation of a large molecule is slower than a smaller atom as expected. The temperature dependence of the relaxation behavior shows faster decay of $S(Q, t)$ with increase in temperature. The water relax-

ation dynamics (Figures 2(c) and (d)), on the other hand, show weak dependence on temperature at all length scale. A noticeable difference between RNA and water relaxation is observed as a function of Q. While water shows close to linear decay pattern with Q, RNA shows variation in decay rates. Later, we will discuss this in more detail.

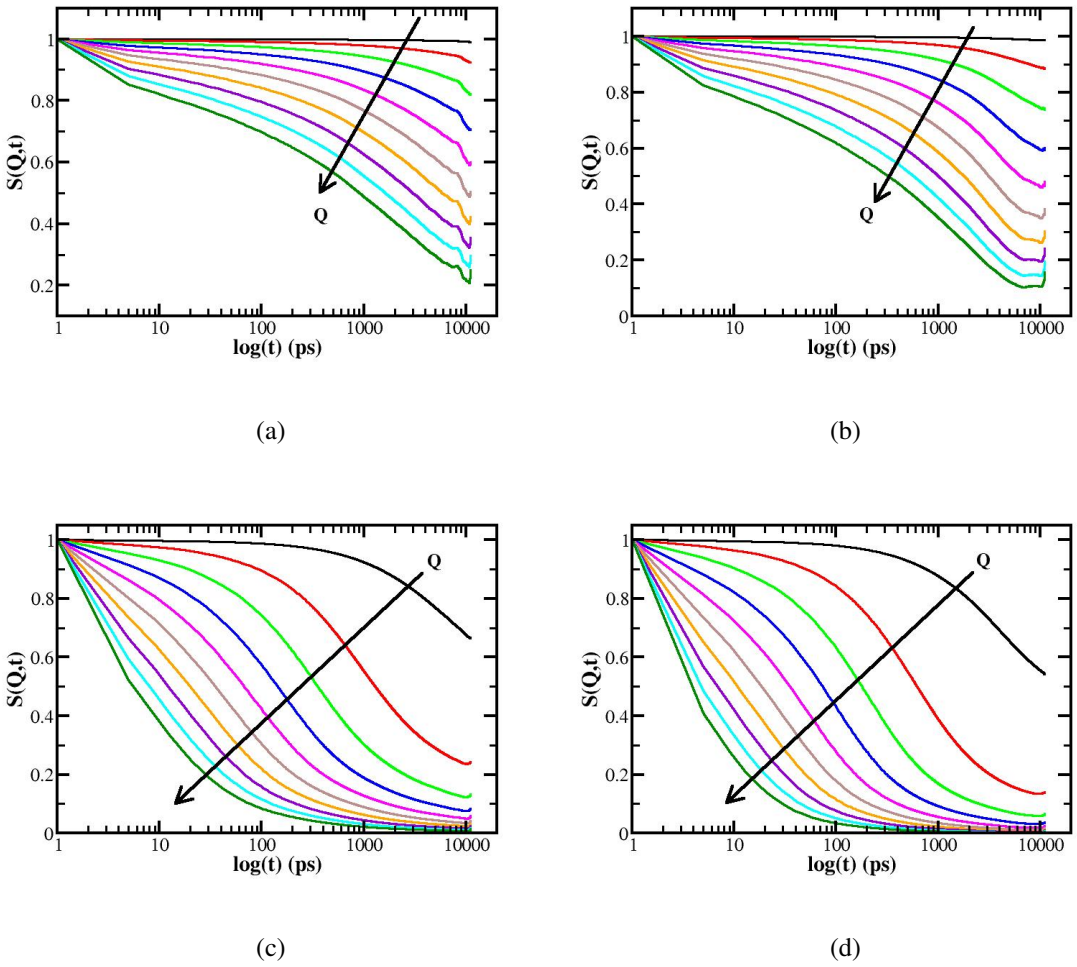

FIG. 2. Intermediate scattering function, $S(Q,t)$ for, (a) RNA at $T = 270K$ and (b) RNA at $T = 300K$. (c) and (d) $S(Q,t)$ for water at $T = 270K$ and $300K$ respectively. Q values are shown from 0.1Å (black line) to 1.9Å^{-1} (green line) at an increasing step of 0.2Å^{-1} to demonstrate the length scale dependence of the structural relaxation. The arrow direction represents increasing Q.

The mean square displacement of the RNA, $< u^2 >$, is estimated from the simulated $S(Q,t)$ using the Gaussian approximation [37, 38], $\langle u^2(T)\rangle = -3Q^{-2}\ln\left[S(Q,t\to\infty)\right]$. The $< u^2 >$ values are shown in Figure 3 ranges from below the freezing temperature, $T = 260K$, to well above freezing temperature, i.e., $300K$. The $< u^2 >$ shows a monotonous increase with tem-

perature. The smooth monotonous increase exemplifies the lack of water crystallization in the hydrated RNA sample at this hydration level, $h = 0.5$. The lack of crystallization was also observed in QENS experiments on transfer-RNA (tRNA) [12] well above the present hydration level up to $h \approx 0.65$. While no signature of crystallization is observed at hydration level, $h = 0.5$, water crystallization was reported earlier [39, 40] for lysozyme at $h \approx 0.5$. This is due to the fact that RNA adsorbs and binds more water molecules than lysozyme due to larger hydrophilic surface area and there are more open structures in RNA compared to lysozyme. The binding of water molecules on the larger hydrophilic surface area of RNA to an open configuration hinders water crystallization. Later, we will discuss the binding of water molecules to the RNA surface in connection with slow and fast water dynamics.

Figure 3 shows the MSD of RNA in the temperature range, $T = 260-300K$. These simulations are performed above the dynamical transition temperatures, T_D as our interest here to understand the difference between RNA and water dynamics beyond T_D. It should be noted, that the MSD shows a slight deviation from a smooth linear increase between $T = 270K$ and $280K$. Slow water molecules that are strongly bound to ionic groups within the RNA are considered part of the biological complex. Hence, the kink observed near $270K$ can be thought of as the stiffening of the RNA due to water confinement below freezing temperature. In a recent experimental work by Zaccai et al. [41], a flatter MSD below $273K$ is observed which the authors argue due to the freezing of free water molecule that may cause stiffening of the ribosome subunits at these low temperatures.

Relaxation dynamics derived from $S(Q,t)$ are slower for RNA compared to water, as shown in Figures 4 and 5. The decay of $S(Q,t)$ of RNA and water as a function of time follows two different power laws. The RNA $S(Q,t)$ shows a stretched exponential or Kohlrausch-William-Watts (KWW) time dependence $S(Q,t) \approx \exp[-(t/\tau)^{\beta}]$, where τ and β are relaxation time and stretching exponent respectively. Water $S(Q,t)$ shows a double exponential decay of the form, $S(Q,t) \approx \exp(-t/\tau_1) + \exp(-t/\tau_2)$, where τ_1 and τ_2 are two time-scales representing slow and fast ($\tau_1 > \tau_2$) relaxations respectively. Relaxation times for all temperatures and Q-values are extracted from the fits. The characteristic relaxation is both a temperature (T) and spatial length-scale (Q) dependent phenomena, as can be seen from the $S(Q,t)$ plots in Figures 4 and 5.

First we examine the RNA characteristic relaxation, shown in Figure 4. In neutron experiments, spatial scales dependence are obtained from the momentum transfer (Q) dependence. Similarly, we examine the spatial dependence (Q-dependence) of relaxation time in Figure 4. The black

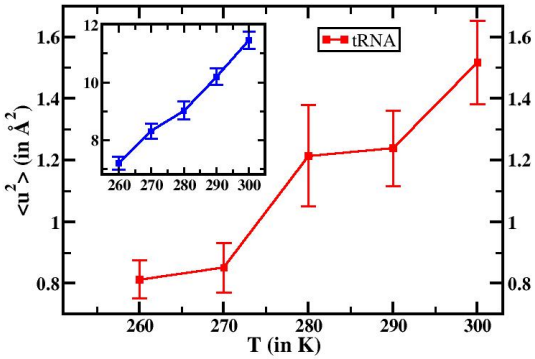

FIG. 3. MSD derived from simulated $S(Q,t)$ using the Gaussian approximation. The error bars are also displayed by up-down lines. The connected lines are for guidance only. For reference, the MSD for deuterated water molecules, similarly derived, are shown in the inset.

lines through the $S(Q,t)$ curves in Figure 4(a) and (b) for temperatures $T = 270K$ and $300K$ show excellent stretched exponential fits for all Q-values. Note that the fitting for $T = 300K$ at long times do not follow stretch exponential type decay in a strict sense. This discrepancy can be related to high temperature relaxation of RNA with water molecules following a fluid-like exponential decay rather than a stretched exponential decay. Also, we have not shown the data for $T = 260K$ in these plots, as $T = 260K$ is well below freezing temperature, and hence the dynamics at this temperature can be questionable due to equilibration issue at low temperature. The relaxation time, τ, and the stretching exponent, β as a function Q for all temperatures are shown in Figures 4(c) and (d). The τ and β values are obtained from the stretched exponential fit of the intermediate scattering function, $S(Q,t)$. In highly confined soft materials, especially in supercooled polymeric system, the relaxation time follows the power-law [29, 30], $\tau \sim Q^{-2/\beta}$, where β ranges from 0 to 1.0. The β values reveal the presence or absence of confinement in the dynamical system. Lower and higher β values refer to strong and weak scaling behaviors respectively and are related to strong and weak confinement. $\beta \sim 1.0$ refers to Fickian diffusion whereas $\beta \sim 0.5$ represents strong scaling with higher confinement. Also, in polymeric systems, $\beta < 1.0$ shows dynamical behaviors refereing to, (i) heterogeneous dynamics related to a distribution of normal diffusion processes having different relaxation time and (ii) homogeneous dynamics that reflects non-exponential behavior in a single relaxation process, typically in the sub-diffusive regime. In Figure 4(d), we observe β values ranging from 0.37 to 0.48 at the low temperature, $T = 270K$,

and from 0.38 to 0.53 at high temperature $T = 300K$. In previous incoherent neutron experiments, strong scaling behavior was observed for a variety of polymeric systems and it was attributed to the anomalous diffusion related to a homogeneous system [30, 42, 43], and is an intrinsic property of homogeneous media. On the other hand, it has also been observed that relaxation times, due to local molecular motion, show heterogeneity in spatial length scales [44–48] in biological interfaces. The stretching exponents in Figure 4(d), show stronger scaling behavior than polymeric systems as can be seen from the β values smaller than or close to 0.5. We fitted the τ versus Q data in Figure 4(c) with $\tau \sim Q^{-2/\beta}$ to obtain the scaling behavior from the relaxation time directly. The results show strong scaling exponent that ranges from $\beta = 0.55$ at $T = 270K$ to $\beta = 0.57$ at $T = 300K$. From Figure 4(d), we find that β values vary in the spatial scales ranging from $Q = 0.1$ to $Q = 2.0$, i.e., $\ell = 62.83$Å to 3.14Å, representing simulation box length-scale to the molecular length-scale. Therefore, the stronger scaling behavior in association with spatial scale, Q, dependence of β values manifest confined and heterogeneous RNA dynamics. Relaxation at the atomic (Angstrom) length-scale is much faster compared to the RNA molecular (Nanometer) length-scale. We therefore, argue that the hydrated RNA relaxation dynamics is heterogeneous due to motion at different length-scales and confined due to strong electrostatic interactions between hydrophilic water molecules. Single molecule studies on many common branched RNA exhibited confined heterogeneous dynamics [49–53].

Water dynamics and its interactions with biomacromolecules generally plays a critical role in structure, dynamics and function of biological systems [1, 25]. However, in neutron experiments, the water molecules are deuterated to focus on the dynamical properties of biomacromolecules. Hence the dynamics of water molecules are often overlooked. Molecular dynamics simulations can be a convenient way of extracting the dynamics of water in biological systems [15]. In Figures 5(a) and (b), we show the $S(Q,t)$ of deuterated water molecules at two different temperatures, $T = 270K$ and $300K$ at different Q. The water $S(Q,t)$ fits well with a double-exponential of the form, $S(Q,t) \approx \exp(-t/\tau_1) + \exp(-t/\tau_2)$. The two relaxation times, τ_1 and τ_2 as a function of Q, are shown in Figures 5(c) and (d). As the relaxation times are obtained from the double exponential fit, *not* from a stretched exponential, the power law relationship, $t(Q) \approx Q^{-2/\beta}$, cannot be used to describe the Q dependence of water relaxation. Instead, we investigate the Q-dependence of τ_1 and τ_2 based on standard diffusion theory. While stretched exponential fittings of water $S(Q,t)$ [1] in the supercooled regime exist, we follow the pioneering works of double exponential fittings that explain the slow and fast dynamics of solvation water in the hydration shells of biomolecules [54–

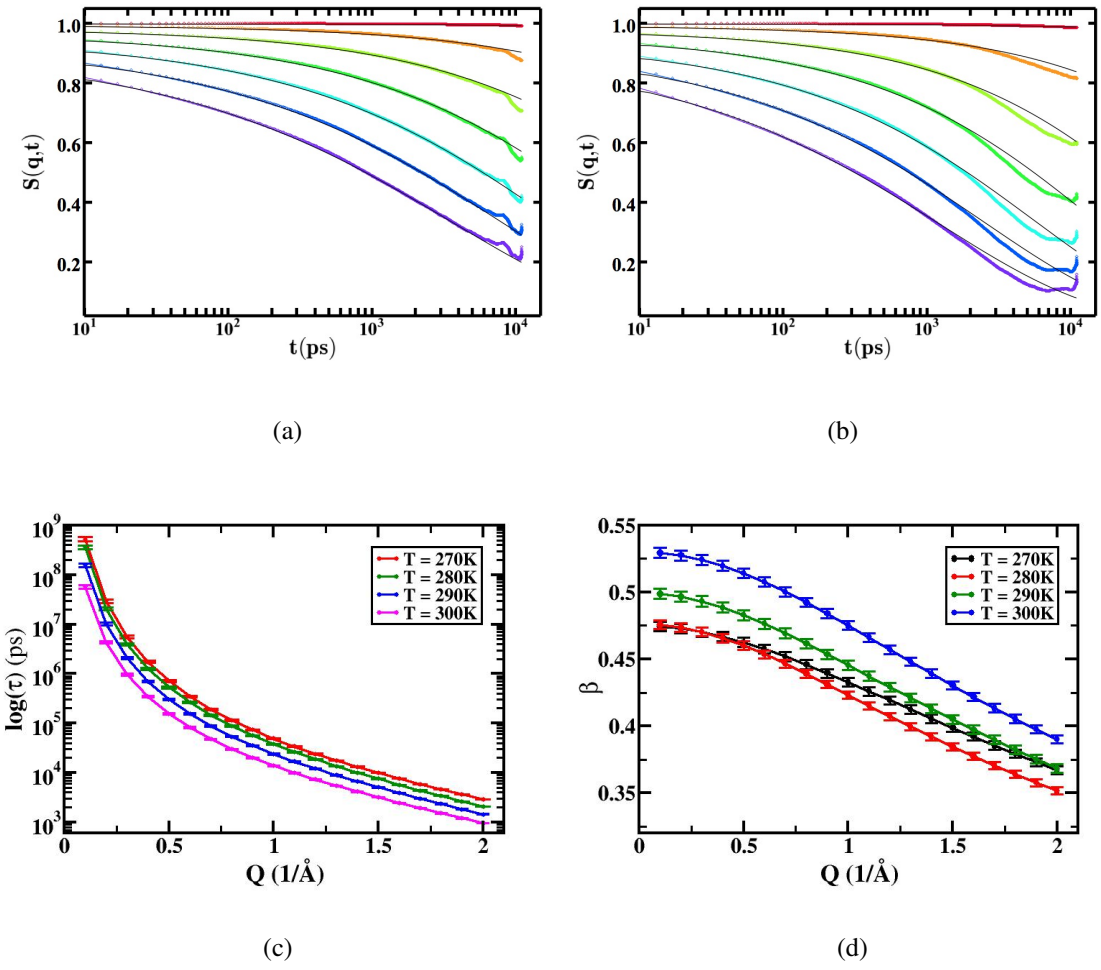

FIG. 4. Stretched exponential fitting of RNA $S(Q,t)$ at, (a) $T = 270K$, and (b) $T = 300K$. From top to bottom $S(Q,t)$ plots represent increasing Q values starting at 0.1Å (red line) at a step of 0.3Å ending at 1.8Å (violet line). The black lines passing through the plots are stretched exponential fits to the data. The bottom panel, (c) and (d) is Q-dependence plots of the relaxation time, τ and the exponent, β of stretched relaxation respectively for all the Q and T values. Lines are guide to the eyes only.

57]. We argue that the water at these temperatures may not be fitted with a stretched exponential as the water cannot be considered supercooled. Instead, the water molecules are confined due to electrostatic interactions between RNA and polar water molecules with dynamics that resembles a non-exponential decay, similar to a collective glassy behavior [58]. We emphasize here that the relaxation process of water is much more complex than that double exponential relaxation and should be characterized by a distribution of relaxation times [59–61]. In Figure 5, relaxation of water molecules show an order of magnitude faster relaxation for fast dynamics (τ_2) compared to

the slow (τ_1). The ultrafast τ_2 relaxation is consistent with earlier observations in biomolecules where the solvation dynamics near proteins were found to be an order of magnitude higher [56]. The slow and fast relaxation rates can be attributed to the water molecules that stay inside the hydration shell of RNA for a prolonged period of time and the water molecules that constantly leave and reenter the hydration shell [1, 55].

In Figures 5(a) and (b), with double exponential fit for $S(Q,t)$ shows that the relaxation becomes faster with increasing Q, however, the double exponential decay of $S(Q,t)$ characteristically remains the same. The Q-dependence of slow and fast relaxations are shown in Figures 5(c) and (d). The Q-dependence of slow relaxation (Figure 5(c)) exhibits around two order of magnitude drop in relaxation times from low to high Q values. This can be attributed to the difference in spatial scale lengths in relaxation of water. For $Q = 0.1\text{Å}^{-1}$, the spatial length scale, $\ell = 62.83\text{Å}$ represent relaxation of water from the entire hydration shell, while for $Q = 1.8\text{Å}^{-1}$, $\ell = 3.5\text{Å}$, and hence the relaxation is solely due to molecular motion of water. The smaller water molecule relaxes faster compared to the entire hydration shell. The second feature extracted from Figure 5(c) shows that the slow relaxation, τ_1, decays exponentially with Q. This type of Arrhenius dependence of τ_1 reflects a strong spatial correlation of slow relaxation. This implies that while the relaxation at the molecular level is faster, the entire hydration shell relaxes slowly, apparently in a clustered or network state [19, 54, 57]. Conversely the prolonged presence of water molecules in the hydration shell generates a strong Q dependence of slow relaxation times [62, 63]. It should be noted, earlier works on water dynamics in the hydration shell around proteins, show strong Q-dependence, but with a power-law dependence for relaxation time derived from susceptibility measurements, instead of Arrhenius-type Q-dependence as observed in this 'slow' relaxation results [63, 64].

The fast relaxing water molecules are not a part of the 'network' in the hydration shell. For these water molecules, diffusion coefficients, D_{fast}, can be obtained from the Q-dependence of relaxation times, as it is done X-ray photon correlation spectroscopy (XPCS) experiments [65]. For typical diffusive water, τ_2 exhibits $1/\tau_2 = Q^2$ behavior in the low-Q regime [57]. Hence, we plot $1/\tau_2$ versus Q^2 in Figure 5(d). The diffusion coefficients obtained from these plots show a narrow range of temperature-dependent diffusivity, from $D_{fast} = 1.17 \times 10^{-6}$ cm^2/sec (for $T = 270K$) to 2.0×10^{-6} cm^2/sec (for $T = 300K$). The D_{fast}, therefore shows order of magnitude slower diffusivity compared to typical diffusion coefficients in bulk water [66–68]. While these water molecules relax faster and enter and leave the hydration shell, the dynamics is confined to

the surface of the RNA molecules and can be considered as part of the interfacial region of the RNA [41, 49]. Hence, the diffusivity can be less than pure bulk water as is observed; an order of magnitude reduction for these simulations.

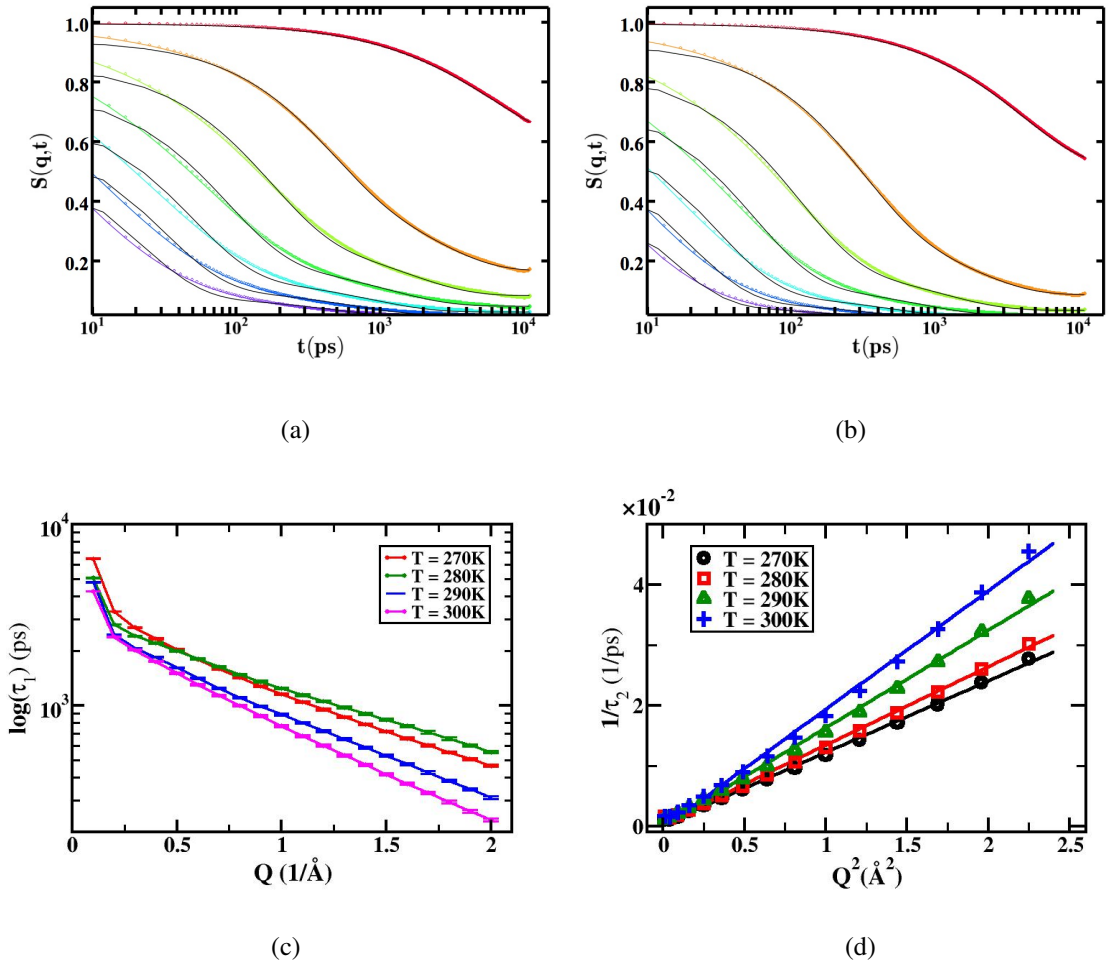

FIG. 5. Fitting of the deuterated water (D_2O) $S(Q,t)$ with a double exponential, (a) $T = 270K$, and (b) $T = 300K$: from top to bottom $S(Q,t)$ plots represent increasing Q values starting at 0.1Å (red line) at a step of 0.3Å ending at 1.8Å (violet line). The black lines passing through the curves represent double exponential fits to the simulated data. (c) Q-dependence plots of the slow relaxation time, τ_1. (d) Fast relaxation time, plotted in $1/\tau_2$, versus Q^2 to show the linear characteristic that helps obtain diffusion constant in the fast relaxation process. For (c) lines are guide to the eyes. (d) the lines are linear fit to the $1/\tau_2$ versus Q^2 data.

The temperature dependence of the relaxation times for RNA and water are shown in Figure 6. The characteristic relaxation time for RNA (Figure 6(a) shows a similar linear decrease

with increasing temperature as observed earlier by Khodadadi et al. [12, 20]. In our simulation we observe a slight discrepancy at between $T = 260K$ to $T = 280K$ where it goes up a small amount from $T = 260K$ and then linearly decreases beyond $T = 270K$. This kink-like behavior betwen $T = 260K$ to $T = 280K$ may be due to a 'stiffening' of the RNA complexes due to freezing of water molecules on the RNA. The stiffening of biomolecules near freezing temperatures have been earlier reported by several authors [41, 69]. The water molecules slow, τ_1, and fast, τ_2, relaxation times as shown in Figure 6(b) and (c), show linear dependence, except in the slow relaxation, τ_1. The slow relaxation remains constant until $T = 280K$, then decreases linearly. The τ_1 is implicative of confined water. It is observed that both of these relaxation times are smaller than RNA. Even the slow water relaxation, τ_1, is $\sim 2 - 3$ order of magnitude faster than the RNA relaxation times (Figure 6(a)). Therefore, we conclude that the confined water is not 'really' bound to the RNA (in which case water and RNA relaxation times would have been comparable to RNA), but these are interfacial waters having strong electrostatic interaction with the RNA . Furthermore, for slow relaxation, the water molecules show very little change in relaxation times below $T = 280K$. We believe that at this low temperature, the water molecules are strongly confined due to electrostatic interactions and hence behave as supercooled water, so the change in relaxation time within the simulation time-frame is very small that can be ignored. To summarize, the characteristic relaxation times of water follow two different relaxation schemes. The interfacial waters are slow moving with a relaxation time 2-3 times faster than the RNA molecules. The fast relaxation, τ_2, implies that the water molecules are bulk-like and move in and out of the solvation shell.

Finally, we present the MSD derived from the time-dependent trajectories ($r_i(t)$) of the 10ns simulations. In Figure 7, we show the MSD defined as, $< \Delta r^2(t) >=< [r(t) - r(0)]^2 >= \frac{1}{N}\sum_{i=1}^{N} < [r_i(t) - r_i(0)]^2 >$, where $r_i(t)$ is the instantaneous positions of the i^{th} molecule at time t. The MSD is derived from the equilibrated MD simulation trajectories (10ns trajectories) and by subtracting the center-of-mass drift motion [70]. In these plots, we calculate the MSD for the hydrogen of RNA molecules and oxygen of water molecules. For water the choice of oxygen dynamics refers to the central atom instead of center-of-mass of the water molecule. As discussed earlier in Figure 1, water molecules are in liquid state at or above $T = 270K$ and also the central simulation cell is relatively small. Therefore, it is hard to distinguish between the water on the RNA surface and bulk water due to the system size effect. We calculated the MSD for all water molecules together, assuming the effect of separating bulk water from surface of RNA would be negligible. The MSD, on a longer time scale, is governed by a power law and given

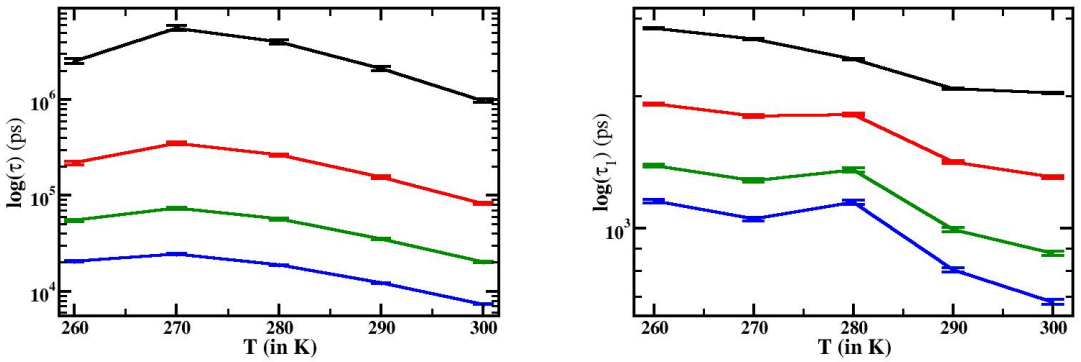

(a)

(b)

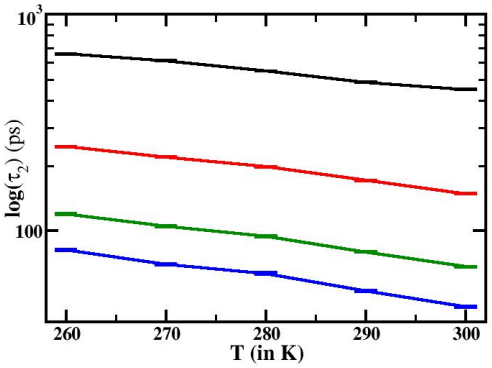

(c)

FIG. 6. Relaxation time as a function of T for four different Q values: 0.3Å^{-1} (black), 0.6Å^{-1} (red), 0.9Å^{-1} (green) and 1.1Å^{-1} (blue) respectively. The corresponding spatial length scales vary from 20.94Å to 5.71Å. (a) RNA relaxation obtained from stretched exponential fit of RNA $S(Q,t)$. (b) and (c) slow and fast relaxation of water obtained from double exponential fit of water $S(Q,t)$. The lines are for guidance only. Error bars show negligible error in our calculation.

by[29], $< \Delta r^2(t) > \propto t^{\alpha}$, where the exponent, α, is a dimensionless number varies from 0 to 2 referring to various diffusive mechanism. The dynamics is categorized for $\alpha < 1$, $\alpha = 1.0$ and $\alpha > 1$ as subdiffusive, diffusive (Brownian) and superdiffusive motions respectively. For the RNA dynamics (Figure 7(a)), two different scalings are observed. While RNA shows subdiffusive dynamics with $\alpha = 2/3$, the water molecules show diffusive motion within the time frame of our simulation. We have not calculated RNA diffusivity from these data due to the subdiffusive nature of the MSD. The RNA dynamics scales with $t^{1/3}$ at shorter times and $t^{2/3}$ at longer times for

these simulations. The RNA diffusion is therefore subdiffusive within the observation time. While the long time effective diffusion constant cannot be measured from the subdiffusive regime, it is important to note that time-dependence diffusivity of the RNA molecules can be obtained from these MSD data. These MSD results prove a key aspect of this study, that the dynamics of RNA and water are decoupled although the water molecules are very close to the RNA surface. While previous neutron scattering experiments [20] in tRNA-water model system show coupled tRNA and hydration water relaxaiton, we have not observed the same. This may be potentially due to the structural differences between the ribozyme and tRNA that have been utilized in these two separate studies. We must also emphasize that observation of water dynamics are straightforward in MD simulations. In neutron scattering with deuterated water though, special care should be taken to calculate water dynamics. In biomolecules, diffusion constant can depend on the observation time and hence diffusivity can be time-dependent [71], i.e., $D(t)$, which is sensitive function of several physical parameters in the biomolecule environment. In Figure 7(b), water MSD show a linear dependence with time. The MSD follows an anomalous region $\alpha < 1.0$ followed by the diffusive regime, $\alpha \approx 0.9$ that is typical to water MSD in hydration shell as has been observed earlier works by several authors [54, 67, 72, 73].

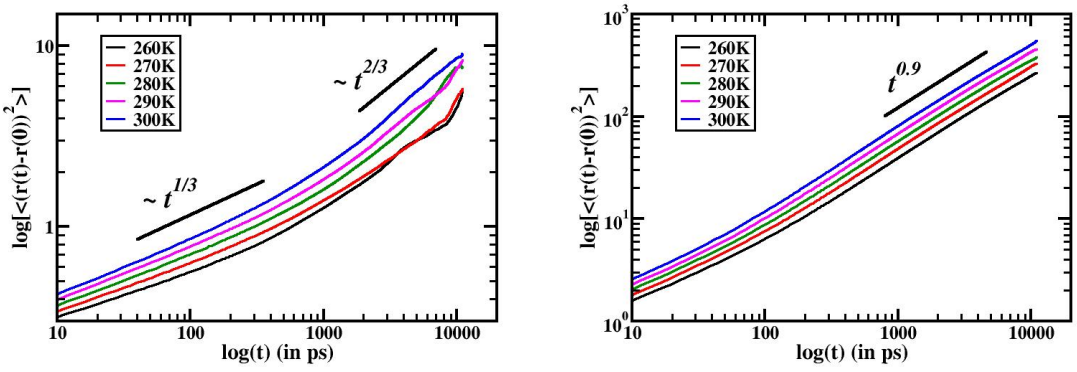

(a) (b)

FIG. 7. Mean-square-displacement (MSD) of RNA and water obtained from the MD trajectories of the RNA and water molecules shown in (a) and (b) respectively. The MSD for RNA is calculated for only hydrogen atoms while the MSD for water is calculated only for Oxygen atoms.

IV. CONCLUSIONS

The structure and dynamics of water inside the hydration shell plays a crucial role in the structure and function of biomolecules. In this article, we show that there is a mismatch between the dynamics of water molecules and the RNA molecules. We examined the dynamics of RNA and water in the hydration shell. RNA and water both show relaxation dynamics dependent on temperature and spatial length-scales. While RNA dynamics can be explained using a stretched exponential decay, relaxation of water follows a double-exponential decay. RNA dynamics show stronger scaling for the relaxation time than typical synthetic polymeric systems. Our observations show that the relaxation of RNA at atomic length scales varies widely compared to the RNA molecular length scales. These results support the assertion that dynamics of solvated RNA is heterogeneous as has been observed by several authors [49–53].

For biomolecular systems, water dynamics is typically overlooked in neutron experiments as water is often deuterated so as to highlight the biomolecular motion. The advantage of the MD simulation is that it does not depend on the low scattering cross section of deuterium, thereby giving us the opportunity to perform a full-scale study of the water molecules. We observed that the motion of the water molecules decays with two characteristic relaxation times, slow, τ_1, and fast, τ_2. Stretched exponential fitting of water $S(Q,t)$ have previously been performed [1] by considering the confined water as supercooled water. We consider the confined water as strongly interacting water with varied relaxation times. The stretched exponential provides only one relaxation time scale and does not explain the different water dynamics in the hydration shell. We believe, that the dynamical behavior of water can be better understood by considering multi-exponential relaxation that can explain the different time scales of water dynamics in the hydration shells. In our simulations, the double exponential fit shows the fast and slow relaxation times that are a many order of magnitude faster than RNA relaxation times. We conclude that the slow and fast relaxations originate from, (1) the interfacial water molecules that are strongly interactive with RNA molecules due to electrostatic interactions, and (2) bulk-like water molecules which leaves and reenter the interfacial region. Our analysis could not confirm the relaxation time scale in which the water molecules are attached to the RNA, in which case the water molecules would have similar relaxation times as RNA.

RNA technology has made an impressive progress in recent years, however, more fundamental understanding of the dynamics of these systems can improve the technology immensely. Our

simulations bridge seemingly disparate observations of similarity of water structures with presence of fast and slow relaxation times well above dynamical transition temperature [19]. We believe this work will provide necessary theoretical background for understanding the fundamental physics behind RNA and water relaxation that can be applied to other biomolecular systems.

V. ACKNOWLEDGEMENTS

This work was supported by the US Department of Energy (DOE), Office of Science, Basic Energy Sciences, Materials Sciences and Engineering Division. NAMD simulations were performed used resources of the Oak Ridge Leadership Computing Facility at the ORNL, which is supported by the Office of Science of the U.S. DOE under Contract No. DE-AC05-00OR22725. Part of this research was conducted at the Center for Nanophase Materials Sciences (CNMS), which is a DOE Science User Facility.

[1] D. Laage, T. Elsaesser, and J. T. Hynes, Chem. Rev. **117**, 10694 (2017).

[2] Y. Levy and J. N. Onuchic, Annu. Rev. Biophys. Biomol. Struct. **35**, 389 (2006).

[3] P. Ball, Chem. Rev. **108**, 74 (2008).

[4] M.-C. Bellissent-Funel, A. Hasanali, M. Havenith, R. Henchman, P. Pohl, F. Sterpone, D. van der Spoel, Y. Xu, and A. E. Garcia, Chem. Rev. **116**, 7673 (2016).

[5] S. Kaieda and B. Halle, J. Phys. Chem. B **117**, 14676 (2013).

[6] D. Laage, G. Stirnemann, F. Sterpone, R. Rey, and J. T. Hynes, Annu. Rev. Phys. Chem. **62**, 395 (2011).

[7] P. Kührova, M. Otyepka, J. Šponer, and P. Baniáš, J. Chem. Theory and Comput. **10**, 401 (2014).

[8] I. D. Kuntz, Adv. Protein Chem. **28**, 239 (1974).

[9] B. Bagchi, Chem. Rev. **105**, 3197 (2005).

[10] R. Kanasty, J. R. Dorkin, A. Vegas, and D. Anderson, Nat. Mater. **12**, 967 (2013).

[11] P. Guo, Nat. Nanotechnol. **5**, 833 (2010).

[12] J. H. Roh, R. M. Briber, A. Damjanovic, D. Thirumalai, S. A. Woodson, and A. P. Sokolov, Biophys. J. **96**, 2755 (2009).

[13] E. H. Grant, R. J. Sheppard, and G. P. South, *Dielectric Behavior of Biological Molecules in Solution* (Clarendon, Oxford, U.K., 1978).

[14] S. Bhattacharyya, Z.-G. Wang, and A. Zewail, J. Phys. Chem. B **107**, 13218 (2003).

[15] G. K. Dhindsa, D. Bhowmik, M. Goswami, H. O'Neil, E. Mamontov, B. G. Sumpter, L. Hong, P. Ganesh, and X. q. Chu, J. Phys. Chem. B **120**, 10059 (2016).

[16] H. Frauenfelder, P. W. Fenimore, and B. H. McMahon, Biophys. Chem. **98**, 35 (2002).

[17] G. Caliskan, D. Mechtani, J. H. Roh, A. Kisliuk, A. P. Sokolov, S. Azzam, M. T. Cicerone, S. Lin-Gibson, and I. Peral, J. Chem. Phys. **121**, 1978 (2004).

[18] P. W. Fenimore, H. Frauenfelder, B. H. McMahon, and F. G. Parak, Proc. Natl. Acad. Sci. **99**, 16047 (2002).

[19] H. Zhang, S. Khodadadi, S. L. Fiedler, and J. E. Curtis, J. Phys. Chem. Lett. **4**, 3325 (2013).

[20] S. Khodadadi, J. H. Roh, A. Kisliuk, E. Mamontov, M. Tyagi, S. A. Woodson, R. M. Briber, and A. P. Sokolov, Biophys. J. **98**, 1321 (2010).

[21] W. Doster, S. Cusach, and W. Petry, Nature **337**, 754 (1989).

[22] M. G. Mazza, K. Stokely, S. E. Pagnotta, F. Bruni, H. E. Stanley, and G. Franzese, Proc. Natl. Acad. Sci. **108**, 19873 (2011).

[23] M. A. Ditzler, M. Otyepka, J. Šponer, and N. G. Walter, Acc. Chem. Res. **43**, 40 (2010).

[24] M. Tarek, G. J. Martyna, and D. J. Tobias, J. Am. Chem. Soc. **122**, 10450 (2000).

[25] G. Caliskan, R. M. B. adn D. Thirumalai, V. Garcia-Sakai, S. A. Woodson, and A. P. Sokolov, J. Am. Chem. Soc. **128**, 32 (2006).

[26] D. Vural, *Dynamics and Dynamical Transistions in Protein*, Ph.D. thesis, University of Delaware (2014).

[27] M. Bee, *Quasielastic Neutron Scattering, Principles and Applications in Solid State Chemistry, Biology and Materials Science* (Taylor & Francis, 1988).

[28] X. q Chu, E. Fratini, P. Balioni, A. Faraone, and S.-H. Chen, Phys. Rev. E **77**, 011908 (2008).

[29] R. Kimmich, *Principles of Soft-Matter Dhyamics, Basic Theories, Non-invasive Methods, Mesoscopic Aspects* (Springer, New York, 2012).

[30] P. Heitjans and J. Karger, *Diffusion in Condensed Matter: Methods, Materials, Models* (Springer, New York, 2005).

[31] J. C. Phillips, R. Braun, W. Wang, J. Gumbart, E. Tajkhorshid, E. Villa, C. Chipot, R. D. Skeel, L. Kale, and K. Schulten, J. Comput. Chem. **26**, 1781 (2005).

[32] B. R. Brooks, C. L. B. III, A. D. M. Jr, L. Nilsson, R. J. Petrella, B. Roux, Y. Won, G. Archontis, C. Bartels, S. Boresch, A. Caflisch, L. Caves, Q. Cui, A. Dinner, M. Feig, S. Fischer, J. Gao, M. Hodoscek, W. Im, K. Kuczera, T. Lazaridis, J. Ma, V. Ovchinnikov, E. Paci, R. Pastor, C. Post, J. Pu, M. Schaefer, B. Tidor, R. M. Venable, H. L. Woodcock, X. Wu, W. Yang, D. York, and M. Karplus, J. Comput. Chem. **30**, 1545 (2009).

[33] W. L. Jorgensen, J. Chandrasekhar, J. D. Madura, R. W. Impey, and M. L. Klein, J. Chem. Phys. **79**, 926 (1983).

[34] T. Róg, M. K. Hinsen, and G. R. Kneller, J. Comp. Chem. **24**, 657 (2003).

[35] W. Humphrey, A. Dalke, and K. Schulten, J. Mol. Graph. **14**, 33 (1996).

[36] P. Auffinger and E. Westhof, Biopolymers **56**, 266 (2001).

[37] A. Rahman, K. S. Singwi, and A. Sjölander, Phys. Rev. **126**, 986 (1962).

[38] G. Zaccai, J. Non-Cryst. Solids **357**, 615 (2011).

[39] J. H. Roh, J. E. Curtis, S. Azzam, V. N. Novikov, I. Peral, Z. Chowdhuri, R. B. Gregory, and A. P. Sokolov, Biophys. J. **91**, 2573 (2006).

[40] J. H. Roh, V. N. Novikov, R. B. Gregory, J. E. Curtis, Z. Chowdhuri, and A. P. Sokolov, Phys. Rev. Lett. **95**, 038101 (2005).

[41] G. Zaccai, F. Natali, J. Peters, M. Řihová, E. Zimmerman, J. Ollivier, J. Combet, M.-C. Maurel, A. Bashan, and A. Yonath, Sci. Reports **6**, 37138 (2016).

[42] A. Arbe, J. Colmenero, M. Monkenbusch, and D. Richter, Phys. Rev. Lett. **81**, 590 (1998).

[43] A. Arbe, J. Colmenero, M. Monkenbusch, and D. Richter, Phys. Rev. Lett. **82**, 1336 (1999).

[44] B. Schiener, R. Bohmer, A. Loidl, and R. V. Chamberlin, Science **274**, 752 (1996).

[45] R. Bohmer, G. Hinze, G. Diezemann, B. Geil, and H. Sillescu, Europhys. Lett. **36**, 55 (1996).

[46] A. Heuer, M. Wilhelm, H. Zimmermann, and H. W. Spiess, Phys. Rev. Lett. **75**, 2851 (1995).

[47] A. Heuer and H. W. Spiess, Phys. Rev. Lett. **82**, 1335 (1999).

[48] S. Pronk, E. Lindahl, and P. M. Kasson, Nat. Commun. **5**, 3034 (2014).

[49] J. Yoon, J.-C. Lin, C. Hyeon, and D. Thirumalai, J. Phys. Chem. B **118**, 7910 (2014).

[50] J. A. Esteban, A. R. Banerjee, and J. M. Burke, J. Biol. Chem. **272**, 13629 (1997).

[51] J. A. Esteban, N. G. Walter, G. Kotzorek, J. E. Heckman, and J. M. Burke, Proc. Natl. Acad. Sci. **95**, 6091 (1998).

[52] X. W. Zhuang, H. D. Kim, M. J. B. Pereira, H. P. Babcock, N. G. Walter, and S. Chu, Science **296**, 1473 (2002).

[53] S. D. Verma, V. Bout, A. David, and M. A. Mark, J. Chem. Phys. **143**, 024110 (2015).

[54] A. R. Bizzarri and S. Cannistraro, J. Phys. Chem. B **106**, 6617 (2002).

[55] V. A. Makarov, B. K. Andrews, P. E. Smith, and B. M. Pettitt, Biophys. J. **79**, 2966 (2000).

[56] L. Zhang, L. Wang, Y.-T. Kao, W. Qiu, O. Okobiah, and D. Zhong, Proc. Nat. Acad. Sci. **104**, 18461 (2007).

[57] F. Perakis, K. Amann-Winkel, F. Lehmkuhler, M. Sprung, D. Mariedahl, J. A. Sellberg, H. Pathak, A. Spah, F. Cavalca, D. Schlesinger, A. Ricci, A. Jain, B. Massani, F. Aubree, C. J. Benmore, T. Loerting, G. Grubel, L. G. M. Petterson, and A. Nilsson, Proc. Nat. Acad. Sci. **114**, 8193 (2017).

[58] P. Kumar, Z. Yan, L. Xu, M. G. Mazza, S. V. Buldyrev, S.-H. Chen, S. Sastry, and H. E. Stanley, Phys. Rev. Lett. **97**, 177802 (2006).

[59] L. Garcia-Tarres and E. Guardia, J. Phys. Chem. B **102**, 7448 (1998).

[60] A. E. Garcia and L. Stiller, J. Comp. Chem. **14**, 1396 (1993).

[61] C. Rocchi, A. R. Bizzarri, and S. Cannistraro, J. Mol. Chem. **14**, 1396 (1993).

[62] A. Oleinikova, N. Smolin, and I. Brovchenko, Biophys. J. **93**, 2986 (2007).

[63] J. D. Nickel, H. H'Neill, L. Hong, M. Tyagi, K. L. Weiss, Z. Yi, E. Mamontov, J. C. Smith, and A. P. Sokolov, Biophys. J. **103**, 1566 (2012).

[64] L. Hong, N. Smolin, B. Linder, A. P. Sokolov, and J. C. Smith, Phys. Rev. Lett. **107**, 148102 (2011).

[65] G. Grubel and F. Zontone, Alloys Compd. **362**, 3 (2004).

[66] P. Mark and L. Nilsson, J. Phys. Chem. A **105**, 9954 (2001).

[67] M. Marchi, F. Sterpone, and M. Ceccarelli, J. Am. Chem. Soc. **124**, 6787 (2002).

[68] B. Bagchi, Chem. Rev. **105**, 3197 (2005).

[69] F.-X. Gallat, A. Laganowsky, K. Wood, F. G. L. van Eijck, J. Wuttke, M. Moulin, M. Hartlein, D. Eisenberg, J.-P. Colletier, G. Zaccai, and M. Welk, Biophys. J. **103**, 129 (2012).

[70] D. Vural, L. Hong, J. C. Smith, and H. R. Glyde, Phys. Rev. E **88**, 052706 (2013).

[71] L. L. Latour, K. Svoboda, P. A. Mitra, and C. H. Sotak, Proc. Natl. Acad. Sci. **91**, 1229 (1994).

[72] A. R. Bizzarri and S. Cannistraro, Phys. Rev. E **53**, R3040 (1996).

[73] F. Pizzitutti, M. Marchi, F. Sterpone, and P. J. Rossky, J. Phys. Chem. B **111**, 7584 (2007).